Tunable ferromagnetism in Ni_{0.97-y}Mn_{y}O thin films with hole doping and their electronic structures

Yuan-Hua Lin, M. Kobayashi, Rongjuan Zhao, G. S. Song, Ce-Wen Nan, Shun Li, Wen-Sheng Yan, J. I. Hwang, Y. Ooki, A. Fujimori, Y. Takeda, S. I. Fujimori, K. Terai, T. Okane, Y. Saitoh, H. Yamagami, and Chen Gao

Phys. Rev. B **83**, 193105 — Published 19 May 2011

DOI: 10.1103/PhysRevB.83.193105

Tunable ferromagnetism in $Ni_{1-x}Mn_xO$ thin films with hole doping and their electronic structures

Yuan-Hua Lin,[1] M. Kobayashi,[2] Rongjuan Zhao,[1] G. S. Song,[2] Ce-Wen Nan,[1*] Shun Li[1], Wen-Sheng Yan[3], J. I. Hwang,[2] Y. Ooki,[2] A. Fujimori,[2] Y. Takeda,[4] S. I. Fujimori,[4] K. Terai,[4] T. Okane,[4] Y. Saitoh,[4] H. Yamagami[4], Chen Gao[3]

1 State Key Laboratory of New Ceramics and Fine Processing, Department of Materials Science and Engineering, Tsinghua University, Beijing 100084, P. R. China

2 Department of Physics, University of Tokyo, 7-3-1 Hongo, Bunkyo-ku, Tokyo 113-0033, Japan

3 National Synchrotron Radiation Laboratory, University of Science and Technology of China, Hefei 230029, P. R. China

4 Synchrotron Radiation Research Unit, Japan Atomic Energy Agency, Sayo-gun, Hyogo 679-5148, Japan

Abstract: We report *p*-type $Li_yNi_{0.97-y}Mn_{0.03}O$ thin films (LNMO) via a simple solution method on silicon substrates. Magnetization measurements reveal that room-temperature tunable ferromagnetism can be observed in these LNMO thin films. The Mn $L_{2,3}$ X-ray absorption and core-level photoelectron spectra indicate that Mn consists of the Mn^{2+} and Mn^{3+} components. The O *K*-edge X-ray absorption spectroscopy reveals that the majority of holes introduced by the Li doping have mainly O 2*p* character, and the hole concentration can be enhanced by almost 2 orders of magnitude by the Li doping, which can tune magnetism and T_C. This ferromagnetic behavior in these LNMO thin films may be ascribed to the effective carrier-induced ferromagnetism (*p*-*d* exchange interaction through the O 2*p* band).

PACS number(s): 75.50.Pp, 75.60.-d, 78.70.Dm

Dilute magnetic semiconductors (DMS) have charge and spin degrees of freedom in a single substance, and attract considerable research due to their high potential for applications in spin-dependent semiconductor electronics.[1] Practical spintronic devices require DMS materials that allow electrons and holes of well-defined and long-lived spin states to be generated, injected into useful structures and controlled at ambient temperature. Especially, the DMS materials should have high Curie temperatures (T_C), high spin polarization of the charge carriers, and compatibility with the semiconductors.[2,3] Spintronic applications require that ferromagnetism has an intrinsic origin, i.e., not from magnetic transition metal (TM) clusters or impurity phases. Recently, a lot of previous theoretical calculations and experimental work on design and exploration of oxide-based DMS or dilute magnetic insulator (DMI) (e.g., various TM ions doped ZnO, TiO_2, In_2O_3, SnO_2, NiO) have been reported for their wide band gap for applications with short wavelength light,[4-8] high T_C exceeding room temperature, and good physical and chemical stability. Sato *et al*.[9] used first-principle calculations to reveal that Mn-doped ZnO changed its magnetic state from the spin-glass state to the FM state as a function of carrier density. Dietl *et al*.[10] used Zener's model to predict some high T_C DMS materials such as GaN and ZnO containing 5% of Mn with a high hole concentration, and revealed that ferromagnetism can be driven by exchange interaction between hole charge carriers and localized spins. Spaldin *et al*.[11] predicted that *p*-type doping in (Zn, Co)O could strongly stabilize the FM state by the density-functional theory approach.

Normally, DMS materials consist of non-magnetic semiconducting materials and impurity magnetic cations. For *p*-type DMS, Magnetic coupling interactions can occur via *p-d* or *d-d* exchange and lead to anitferromagnetic or ferromagnetic coupling, which depends on the concentration and the localized spin structural environment of the magnetic impurity.[12,13] Ferromagnetic behaviors of TM-doped oxides-based films are intimately

correlated with the local structural defects, carrier concentrations, electronic structure, coupling between localized magnetization, etc.[14-17] Although many experimental data and corresponding mechanism have been proposed for understanding the intrinsic magnetic ordering in these oxides-based DMS, the origin of ferromagnetic behaviors in these oxides has still been matter of strong debate.[18]

Compared to the TM-doped ZnO, TiO_2, and SnO_2 systems, which are *n*-type DMSs, it is more feasible to realize the *p*-type doping in NiO system, which could become FM from AFM by doping.[19,20] Thus, NiO can be a good room-temperature *p*-type DMS. However, what is the mechanism behind and how to tune FM properties of p-type NiO DMS are still unclear. In this work, we report Li and Mn co-doped NiO thin films ($Li_yNi_{0.97-y}Mn_{0.03}O$, y = 0-0.10, abbreviated as LNMO) via a simple sol-gel spin-coating method on Si substrates. Magnetization measurement reveals that all of these LNMO thin films show room-temperature ferromagnetic properties, which can be effectively tuned by the addition of Li. Our observations demonstrate that NiO-based thin films can be a class of promising *p*-type Oxide-based DMS at room temperature.

Three kinds of LNMO thin films (50 ~ 80 nm thickness) with nominal compositions of $Ni_{0.97}Mn_{0.03}O$ (LNMO-1), $Li_{0.04}Ni_{0.93}Mn_{0.03}O$ (LNMO-2), $Li_{0.10}Ni_{0.87}Mn_{0.03}O$ (LNMO-3), were prepared on Pt(111)/Ti/SiO_2/Si (100) substrates by a sol-gel process and rapid thermal annealing as previously reported.[19] Magnetic measurements were examined using a superconducting quantum interference device (SQUID) and a vibrating-sample magnetometer (VSM) in a temperature range of 300-600 K. X-ray absorption spectroscopy (XAS) measurements were performed at the soft x-ray beam line BL23SU of SPring-8.[20] The monochromator resolution was $E/\Delta E$> 10,000. XAS signals were measured by the total electron yield method. X-ray photoemission spectroscopy (XPS) measurements were performed using a Gamma data Scienta SES-100 hemispherical analyzer and a Mg-$K\alpha$

source ($h\nu$ = 1253.6 eV) in a vacuum below 1.0×10^{-7} Pa. All the measurements were done at room temperature in the base pressure below 1.0×10^{-7} Pa. For surface cleaning, Ar^+ ions puttering and annealing under oxygen pressure ~10^{-4} Pa were performed. Cleanness of the surface was checked by the absence of a high binding-energy shoulder in the O 1*s* XPS core-level spectrum and the C core-level 1*s* contamination signal.

The resultant LNMO thin films are of the single-phase rock-salt structure determined by XRD with a θ-2θ scan and High-resolution TEM (not presented here). Figure 1 shows the magnetization-field (M-H) curves of the LNMO thin films at room temperature. The results indicate that the magnetization can be enhanced significantly by Li co-doping, and the saturated magnetization (Ms) of the LNMO-3 sample (~ 43 emu/cm^3) is about 3 times larger than that of LNMO-1 sample without Li doping. The coercivity is about 128.5, 56.0, and 48.1 Oe for LNMO-1, -2 and -3 samples, respectively, which indicate that the Li doping concentration can also tune the coercivity. The similar behavior was also observed in the Co-doped ZnO films with the addition of Li.[21]

Figure 2 shows the temperature dependence of magnetization for various LNMO thin films. For a random distribution of the localized spins, the Curie temperature T_C of DMS deduced from the Zener model can be mainly correlated to the TM concentration, the hole concentration, the effective spin moment, and the exchange energy between the holes and magnetic ions.[22] T_C obtained from the mean-field theory has the following form:[23]

$$T_C \propto S(S+1)Nm^*p^{1/3} \quad (1)$$

where S is the spin and m^* is the effective mass of the hole. N is the Mn concentration and p is the hole concentration. It is effective in the weak exchange coupling between the localized moments and the band carriers when the concentrations of carriers and localized spins are relatively low. As seen from Fig. 2, we can observe that T_C can be enhanced by about 30 K by 10% Li doping. It should be due to the fact that the Li-doping increases the

hole concentration in NiO-based films, thus enhances the T_C value. The inset in Fig. 3 shows a plot of T_C as a function of $p^{1/3}$ and a linear dependence is apparent.

It is generally believed that XAS is a powerful tool to investigate the electronic structure of oxides materials.[24,25] In order to find the chemical state of the Mn ions, XAS measurements were performed. Figure 3 shows Mn $L_{2,3}$ XAS spectra of the $Li_yNi_{0.97-y}Mn_{0.03}O$ thin films. The line shapes of the Mn $L_{2,3}$ spectra are similar among them, but the ratio of the intensity of peaks at $hv \sim 642$eV to that at ~ 640 eV increases with increasing Li content. The positions of the peaks at $hv \sim 640$ and 642 eV correspond to those of MnO (Mn^{2+}) and $LaMnO_3$ (Mn^{3+}), respectively, as shown in Fig. 3(a). Assuming the spectral changes depending on the Li content are caused by the valence changes of the Mn ions, the spectra can be decomposed by into those of the Mn^{2+} (MnO) and Mn^{3+} ($LaMnO_3$) spectra.[26] The analysis for the $Ni_{0.97}Mn_{0.03}O$ thin film is shown in Fig. 3(b), which indicates that the linear combinations well reproduce the Mn $L_{2,3}$ XAS spectra. The Li-content dependence of Mn valence estimated by the fitting is plotted in Fig. 3(c). Although the Mn^{3+} content is dominant in the $Li_yNi_{0.97-y}Mn_{0.03}O$ films, the Mn^{2+} and the Mn^{3+} content slightly decreases and increases with increasing Li content, respectively. The result indicates that holes induced by the Li doping may change the Mn^{2+} ions to Mn^{3+}. However, the increase of Mn^{3+} content is about 1/20 of the amount of Li content, suggesting that only small part of doped holes are trapped at the Mn^{2+} site. It is likely that the majority of holes enter the Ni 3*d* band and/or is compensated by donor defects such as oxygen vacancies.

In order to reveal the character of the charge compensation states in these LNMO thin films, we measured O *K* XAS spectra for LNMO thin films. Figure 4 shows the O *K*-edge XAS spectra for these LNMO thin films. In the O *K* XAS spectra, the empty O 2*p* states can be probed directly and the Ni 3*d* structure can also be seen because of the ground-state

hybridization between Ni 3*d* and O 2*p*. The peak at 531.2 eV observed in the O *K* edge can be identified as the transition from O 1*s* to Ni 3*d* (d^9) hybridized with O 2*p* as previously reported.[27] The broad peak structure near 536-547 eV can be assigned to O 2*p* character in the Ni 4*s* and 4*p* bands. Considering to neglect the mixing with the $|d^{10}\underline{L}>$ and $|d^{10}\underline{L}^2>$ states due to the large *d*-*d* Coulomb interaction, the ground-state wave function in a cluster approach with Ni in an octahedron of O ions can be simplified as:[28]

$$\Phi_G = \alpha|d^8> + \beta|d^9\underline{L}> \quad (\alpha^2 + \beta^2 = 1) \qquad (2)$$

where $\underline{L}$ stands for an O 2*p* hole. Therefore, the intensity of the 531.2 eV peak in the O *K* spectra should be proportional to β^2. Of interest to note, as the Li doping content increasing, a new peak near 529.1 eV appears in these LNMO thin films, which can be attributed to transitions from O 1*s* to holes doped into the top of the O 2*p* band by Li substitution. The similar spectra behaviors have also been observed by Kuiper *et al*. in Li-doped NiO system.[27,29] As for the sample without Li doping, the final state has no states with lower energy to hybridize. However, as doped with Li, the $d^9\underline{L}$-like final state can hybridize with the lower-energy states where the Li-induced hole is occupied, and such kind of final-state hybridization can shift the spectral weight to the lower-energy state. Additionally, the 529.1 eV prepeak increases obviously with the Li doping content increasing, which imply that the holes introduced by the Li doping should have mainly O 2*p* character. This was also confirmed by the previous bremsstrahlung isochromat spectroscopy (BIS) and XAS spectra.[27,30]

As well known, pure NiO is an antiferromagnetic (AFM) insulator at room temperature, but its conductivity can be tuned by introducing Ni^{2+} vacancies or doping with Li^+.[31] Normally, the competition between ferromagnetic and antiferromagnetic interactions in metals will lead to a spin-glass but not a ferromagnetic ground state. In the case of semiconductors, the mean distance between the carriers is usually much greater than that

between the spins, and thus the exchange interaction mediated by the carriers is ferromagnetic for most of the spin pairs.[32] As shown in Fig. 1, obvious room-temperature FM behaviors can be observed and the magnetization of LNMO increases as the Li-doped concentration increasing. As previously reported, Mn-doped oxide-based DMS systems, the possible presence of a secondary phase (e.g., metallic magnetic Mn clusters) can also be the origin of ferromagnetism. Our XAS results reveal that the secondary Mn metal cluster phase as the origin of ferromagnetism can be ruled out. Therefore, the ferromagnetism in these LNMO thin films is most likely attributed to a carrier-induced mechanism. Hall effects measurements results indicate that the holes are major carriers in these LNMO films and show *p*-type semiconductor. The carrier concentration in LNMO-3 film (~1.7×10^{17} cm^{-3}) can be enhanced by almost 2 orders of magnitude as compared to LNMO-1 film (~5.7×10^{15} cm^{-3}). A ferromagnetic exchange interaction between the magnetic Mn ions and a spin-polarized hole trapped at Ni vacancy can occur. With increasing the Li doping concentration, more hole carriers will be generated. The increased hole carriers are expected to enhance the exchange coupling between the hole carriers and the Mn 3*d* spins, thus make FM coupling interaction more effectively, which gives an obvious enhancement of FM properties for these LNMO thin films. The similar phenomena have also been observed in the Li co-doped ZnO: Co and Cu co-doped ZnO: Fe thin films.[33]

In summary, all of *p*-type LNMO thin films show room-temperature ferromagnetism, and can be tuned by the Li doping. Our XAS experimental data reveal that Mn ions are composed of Mn^{2+} and Mn^{3+} ions, and no metallic Mn observed. The holes compensating the Li doping in LNMO films are located primarily in the O 2*p* states. These holes have a great influence on the Curie temperature and ferromagnetic properties. The observed ferromagnetism in these LNMO thin films may be originated from carrier-induced ferromagnetism.

ACKNOWLEDGMENTS

This work was supported by the Ministry of Sci & Tech of China through a 973-Project, under grant No. 2009CB623303, and NSF of China (50621201 and 10574078), also supported by a Grant-in-Aid for Scientific Research in Priority Area "Invention of Anomalous Quantum Materials" (16076208) from MEXT, Japan. The experiment at SPring-8 was approved by the Japan Synchrotron Radiation Research Institute (JASRI) Proposal Review Committee (Proposal No. 2006A3823). M. K. acknowledges support from the Japan Society for the Promotion of Science for Young Scientists.

Correspondence should be addressed to C. -W. Nan (cwnan@tsinghua.edu.cn).

Refs:

1 H. Ohno, Science 281, 951 (1998)

2 S. A. Wolf, D. D. Awschalom, R. A. Buhrman, J. M. Daughton, S. von Molnar, M. L. Roukes, A. Y. Chtchelkanova, and D. M. Treger, Science 294, 1488 (2001).

3 T. Dietl and H. Ohno, Materials Today, 9, 18 (2006).

4 K. R. Kittilstved, W. K. Liu, D. R. Gamelin, Nature Mater. 5, 291 (2006).

5 W. Prellier, A. Fouchet, B. Mercey, J. Phys. Condens. Matter 15, R1583 (2003).

6 Y.-H Lin, J. Wang, J. Cai, R. Zhao, M. Ying, C.-W Nan, Phys. Rev. B, 73, 193308 (2006); M. Kobayashi, J. I. Hwang, G. S. Song, Y. Ooki, M. Takizawa, A. Fujimori, Y. Takeda, S.-I. Fujimori, K. Terai, T. Okane, Y. Saitoh, H. Yamagami, Y.-H. Lin, and C.-W. Nan, Phys. Rev. B 78, 155322 (2008).

7 J. M. D. Coey, A. P. Douvalis, C. B. Fitzgerald, M. Venkatesan, Appl. Phys. Lett. 84, 1332 (2004).

8 S. J. Pearton, C. R. Abernathy, M. E. Overberg, G. T. Thaler, D. P. Norton, N. Theodoropoulou, A. F. Hebard,Y. D. Park, F. Ren, J. Kim, L. A. Boatner, J. Appl. Phys. 93, 1 (2003).

9 K. Sato, H. K. Yoshida, Semicond. Sci. Technol. 17, 367 (2002).

10 T. Dietl, H. Ohno, F. Matsukura, J. Cibert, and D. Ferrand, Science, 287, 1019 (2000).

11 N. A. Spaldin, Phys. Rev. B 69, 125201 (2004).

12 T. Mizokawa, T. Nambu, A. Fujimori, T. Fukumura, and M. Kawasaki, Phys. Rev. B 65, 085209 (2002).

13 J. M. D. Coey, M. Venkatesan, C. B. Fitzgerald, Nature Mater. 4, 173 (2005).

14 K. R. Kittilstved, W. K. Liu, D. R. Gamelin, Nature Mater. 5, 291 (2006).

15 T. Fukumura, Y. Yamada, H. Toyosaki, T. Hasegawa, H. Koinuma, M. Kawasaki, Appl.

Surf. Sci. 223, 62-67 (2004).

16 J. Philip, A. Punnoose, B. I. Kim, K. M. Reddy, S. Layne, J. O. Holmes, B. Satpati, P. R. Leclair, T. S. Santos and J. S. Moodera, Nature Mater. 5, 298 (2006).

17 M. Kobayashi, Y. Ishida, J. I. Hwang, T. Mizokawa, A. Fujimori, K. Mamiya, J. Okamoto, Y. Takeda, T. Okane, Y. Saitoh, Y. Muramatsu, A. Tanaka, H. Saeki, H. Tabata, and T. Kawai, Phys. Rev. B 72, 201201 (2005).

18 F. Pan, C. Song, X. J. Liu, Y. C. Yang, F. Zeng, Materi. Sci. Eng. R 62, 1 (2008).

19 Y.-H. Lin, R. Zhao, C.-W. Nan, M. Ying, M. Kobayashi, Y. Ooki, and A. Fujimori, Appl. Phys. Lett. 89, 202501 (2006).

20 W. S. Yan, W. Weng, G. Zhang, Z. Sun, Q. Liu, Z. Pan, Y. Guo, P. Xu, S. Wei, Y. Zhang, S. Yan, Appl. Phys. Lett. 92, 052508 (2008).

21 M. H. F. Sluiter, Y. Kawazoe, Parmanand Sharma, A. Inoue, A. R. Raju, C. Rout, and U.V. Waghmare. Phys. Rev. Lett., 94, 187204 (2005).

22 Nicola A. Spaldin.Phys. Rev. B 69, 125201 (2004).

23 C. H. Ziener, S. Glutsch, and F. Bechstedt, Phys. Rev. B 70, 075205, (2004).

24 M. Imada, A. Fujimori, and Y. Tokura, Rev. Mod. Phys. 70, 1039 (1998)

25 F. M. F. de Groot, J. C. Fuggle, B. T. Thole, G. A. Sawatzky, Phys. Rev. B 41, 928 (1990).

26 C. Mitra, Z. Hu, P. Raychaudhuri, S. Wirth, S. I. Csiszar, H. H. Hsieh, H.-J. Lin, C. T. Chen, and L. H. Tjeng, Phys. Rev. B 67, 092404 (2003).

27 J. van Elp, H. Eskes, P. Kuiper, and G. A. Sawatzky. Phys. Rev. B 45,1612 (1992).

28 G. A. Sawatzky and J. W. Allen, Phys. Rev. Lett. 53, 2339 (1984).

29 P. Kuiper, G. Kruizinga, J. Ghijsen, G. A. Sawatzky, H. Verweij, Phys. Rev. Lett. 62, 221 (1989).

30 G. van der Laan, C. Westra, C. Haas, and G. A. Sawatzky, Phys. Rev. B 23,4369 (1981).

31 A. J. Bosman, H. J. Van Daal, Adv. Phys. 19, 1 (1970).

32 T. Dietl, H. Ohno, and F. Matsukura, Phys. Rev. B 63, 195205 (2001).

33 S. J. Han, J. W. Song, C.-H. Yang, S. H. Park, J.-H. Park, and Y. H. Jeong, K. W. Rhie, Appl. Phys. Lett. 81, 4212 (2002).

Figure captions

Fig. 1 Magnetization-field (M-H) loop curves of various $Li_yNi_{0.97-y}Mn_{0.03}O$ thin films; inset is the expand part.

Fig. 2 Temperature dependence of magnetization for $Li_yNi_{0.97-y}Mn_{0.03}O$ thin films; inset is a plot of T_C as a function of hole concentration $p^{1/3}$.

Fig. 3 Mn $L_{2,3}$ XAS spectra of $Li_yNi_{0.97-y}Mn_{0.03}O$. (a) Li concentration dependence. The dashed lines are guide for the eye. (b) Fitting result for the $Ni_{0.97}Mn_{0.03}O$ sample, where the spectrum is assumed to be a superposition of the spectrum of MnO (Mn^{2+}) and that of $LaMnO_3$ (Mn^{3+}) [26]. (c) Mn^{2+} and Mn^{3+} contents plotted as functions of Li content.

Fig. 4 O *K* XAS spectra for $Li_yNi_{0.97-y}Mn_{0.03}O$ thin films.

Authors: *By Y.-H. Lin, et al.*

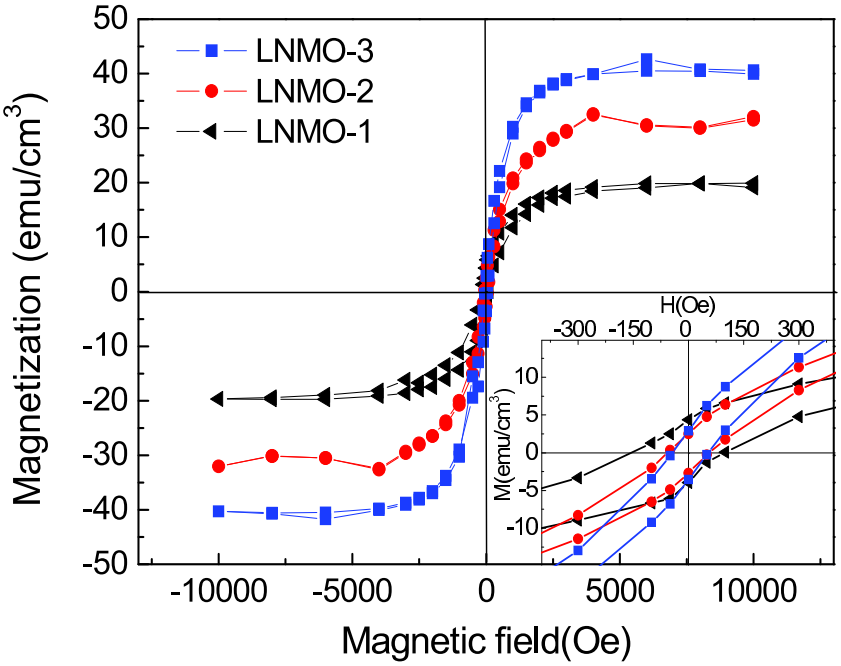

Fig. 1

Figure 1 BAJ1137 07APR2011

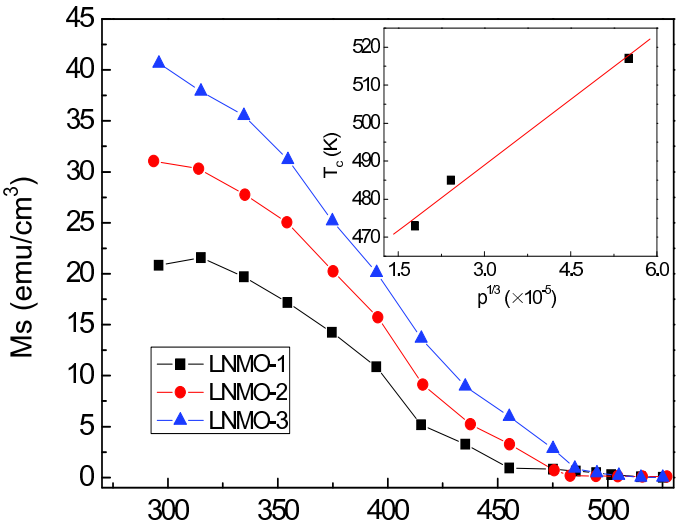

Fig. 2

Figure 2 BAJ1137 07APR2011

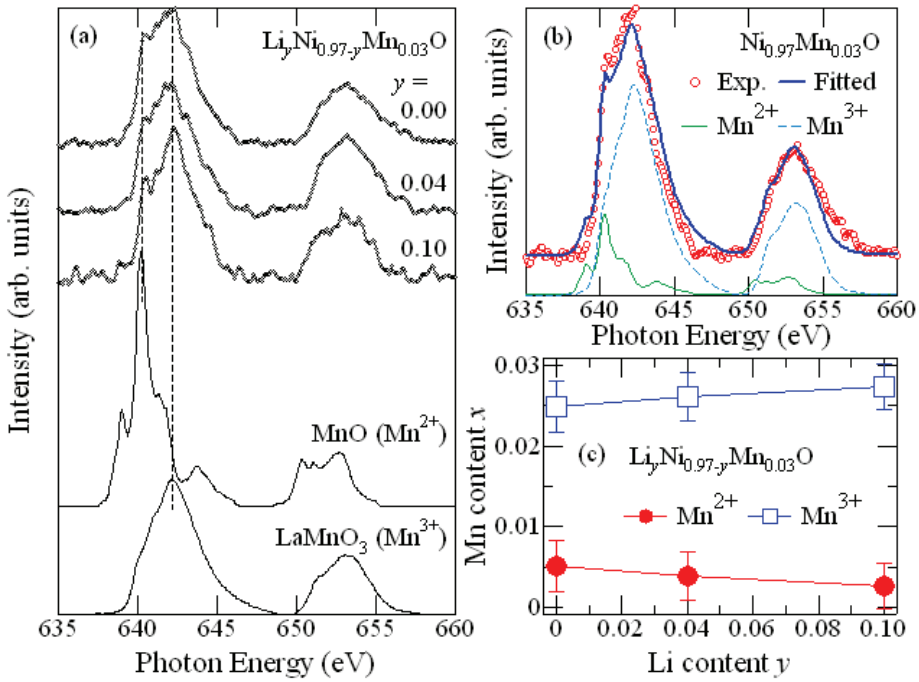

Fig. 3

Figure 3 BAJ1137 07APR2011

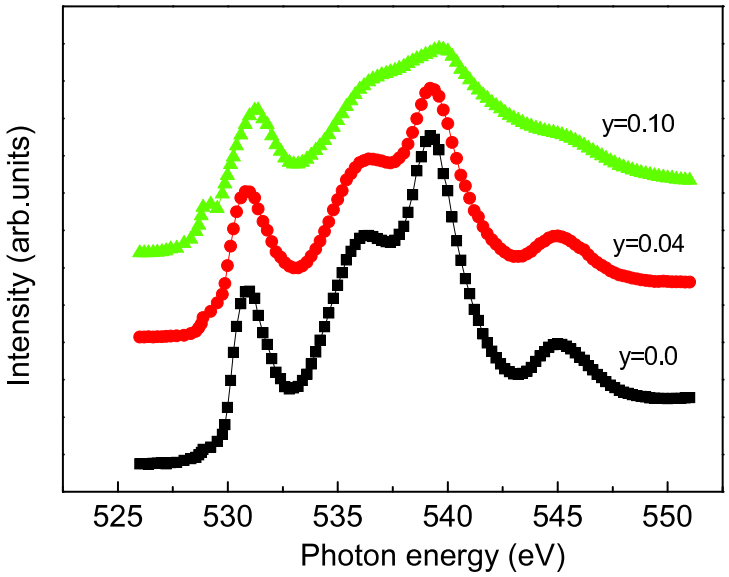

Fig. 4

Figure 4 BAJ1137 07APR2011